Max-Planck-Institut für Mathematik in den Naturwissenschaften Leipzig

Real-Space Mesh Techniques in Molecular Theory of 3D Solvation

by

Gennady Chuev

Preprint no.: 85 2011

Real-Space Mesh Techniques in Molecular Theory of 3D Solvation

Gennady N. Chuev[1,2]

[1] *Max Planck Institute for Mathematics in the Sciences, Inselstrasse 22, Leipzig, 04103, Germany*

[2] *Institute of Theoretical and Experimental Biophysics, Russian Academy of Science, Pushchino, Moscow Region, 142290, Russia*

(Dated: November 18, 2011)

To provide fast computation of the 3D solvation in molecular liquids, we develop a new computational approach based on real-space mesh techniques. Basic aspects and peculiarities of this approach are presented within the framework of the integral equation theory of molecular liquids. Starting from the free energy functional of the 3D solvation problem, we reformulate the integral equations in terms of the solvent induced potential. As a result, we reduce the problem to evaluation of the volume integrals in the interface region. We perform a domain decomposition of the region in terms of finite elements consisting from of the relevant surface elements built from scaled solvent accessible surfaces. The Chebyshev polynomials are found to be the most suitable for accurate approximation of the sought-for functions for these finite elements. The tensor product approximation and the nonequispaced fast fourier transform are proposed to be applied for fast evaluation of the relevant kernel of the integral equations. The computational complexity of the calculations are supposed to be reduced by 10^3 times with respect to current algorithms of the molecular solvation, which are based on the uniform fast fourier transform.

I. INTRODUCTION

Solvation phenomena play a key role in various chemical and biological processes. Many nanotechnological applications are also based on manipulations in molecular or macromolecular solutions. Considerable effort has been devoted to develop efficient computational methods, which are able to reveal mechanisms of the solvation. Although significant progress has been made in the field of computational chemistry in recent decades due to a strong increase in computational resources, the most of investigations of solvation effects are still experimental, whereas successive applications of computational methods are rather limited. The reason of that lies, perhaps, in many-body cooperative nature of the solvation, which requires fine evaluations of the whole system including dozens (or sometimes hundreds) of thousands of molecules. Details of the intermolecular interactions are believed to be investigated in the full format by molecular simulations based on quantum, classical, or hybrid schemes. All these schemes can be broadly classified into two types - continuum and explicit (discrete) solvent models. Continuum methods are computationally efficient,[1–3] but often inadequate to properly represent the specific molecular interactions between the solute and solvent molecules. The discrete molecular mechanics (MM) models are, in principle, more realistic,[4,5] since they treat explicitly intermolecular interactions. However their use dramatically increases the computational time necessary to carry out statistical sampling.

Given the above difficulties, there is an ongoing effort to develop new accurate and efficient solvation models. Among the recent developments in this area is the integral equation theory (IET) of molecular liquids (see, for example Ref.[6]). Similar to explicit solvation models, this approach provides detailed information about intermolecular interactions in terms of solute-solvent distribution functions. Although a considerable progress has been achieved in the development of the IET, nevertheless the application of the theory is still limited in the case of molecular liquids, because the complete treatment of the liquids requires investigations of 6-dimensional distribution functions and solution of the corresponding high-dimensional integral equations. The bottleneck of current algorithms for search of such solution is likely that most of the them are based on the uniform fast fourier transform (FFT) which extension to high dimensions requires to treat enormous large number of grid points. There is a naive idea that a nonuniform distribution of the grid points can significantly reduce computational costs, and hence, increase effectiveness of the calculations. For example, multigrid and

multiscale algorithms have been actively applied to solve the Poisson-Boltzmann equation,[7,8] whereas real space mesh (RSM) techniques have been extensively used to solve the Hartree-Fock and Kohn-Sham equations of electronic structure (see, review[8]). There are also several attempts to apply the algorithms based on multiscale meshes[9] or wavelets,[10] to molecular theory of solvation, however, the comparative analysis[11] does not reveal serious advantages of the methods with respect to the uniform FFT.

Nevertheless, the idea of the RSM techniques remains to be attractive for applications to the IET. However, to realize this approach we are to analyze carefully peculiarities and limitations of the method. The goal of this paper is to provide such analysis and formulate requirements for RSM algorithms which are able to perform effective calculations in the case of three-dimensional (3D) treatment of solvation in molecular liquids. The layout of the paper is the following. First, we outline the IET method in Sec. 2, mainly focusing on the mathematical statement of the 3D solvation problem. We also describe briefly the physical behavior of the sough-for functions, since it is important for a choice of the RSM scheme. Relations between the 3D solvation and other IET approaches to molecular liquids are outlined in the Appendix, where we describe the main scheme of iterative solutions of the relevant integral equations, and indicate bottlenecks in the direct application of RSM to IET of molecular liquids. In Sec. 3, we rewrite the integral equations in the terms of the solvent induced potential, which allows us to reduce the problem to evaluations in a narrow interface region. Then, we apply the basis set representation to the IET (Section 4) and formulate requirements for the application of the RSM techniques to molecular liquids. In Section 4, we perform a domain decomposition of the interface region in terms of spherical shell elements consisting from of the relevant surface elements. These surface elements are supposed to be built from scaled solvent accessible surfaces. Then, we indicate that the Chebyshev polynomials are to be the most suitable for accurate approximation of the sought-for functions for these finite elements. In Section 5, we apply the tensor product approximation and the non-equispaced fast fourier transform (NFFT) to provide effective calculations of the relevant kernels of the integral equations. Finally, we propose to combine fast spherical transform with fast polynomial multiplication to provide NFFT for each finite element. We should remark that we discuss here only the main features of the RSM approach to molecular theory of solvation, while detailed calculations based on this approach will be provided elsewhere.

II. 3D IET OF MOLECULAR LIQUIDS

Integral equations in the 3D format. The IET of molecular liquids provides evaluations of equilibrium solvent densities around molecular solutes, from which various thermodynamic properties may be obtained. The IET method consists in calculations of the binary correlation functions $g(\mathbf{r},\mathbf{\Theta})$ representing the density distributions of molecular species with regards to their translational $\mathbf{r}$ and orientational $\mathbf{\Theta}$ degrees of freedom. The theory is based on the Molecular Ornstein-Zernike (MOZ) integral equation which relates the total correlation function, $h(\mathbf{r},\mathbf{\Theta}) = g(\mathbf{r},\mathbf{\Theta}) - 1$, with the direct correlation functions, $c(\mathbf{r},\mathbf{\Theta})$[12] (see, Appendix). In the general case, the correlation functions are the six-dimensional (6D) functions (distance + 5 independent angles). The high dimensionality of the MOZ equation makes it practically insolvable for most systems of chemical interest. The conventional approximation is to reduce the dimensionality by averaging the functions over angular distributions. In practice, it is performed by averaging the susceptibility around solvent sites. We should remark that although the averaging strongly reduces the dimensionality, it decreases also the quality of molecular representation and produces additional errors, since some molecular information may be lost.

After this averaging the MOZ transforms into the set of 3D Ornstein-Zernike (OZ) integral equations for the relevant 3D correlation functions:[13]

$$h_i(\mathbf{r}) = \sum_{j=1}^{N_v} \int_{\mathbf{R}^3} \chi_{ij}(\mathbf{r}-\mathbf{r}_1) c_j(\mathbf{r}_1) d\mathbf{r}_1, \tag{1}$$

where $\chi_{ij}(\mathbf{r})$ is the 3D matrix of susceptibility (input data). Of course, the averaging procedure increases the number of components up to the number of different solvent sites N_v and typically this number N_v is not so large (does not exceed several units). The reduction of the closure to the 3D case is straightforward (see Appendix), we should replace only 6D variables by their 3D vector analogs. The general form of the closure relation is written as

$$h_i(\mathbf{r}) = \exp[-\beta U_i(\mathbf{r}) + h_i(\mathbf{r}) - c_i(\mathbf{r}) + B_i(h_i - c_i)] - 1, \tag{2}$$

where $U_i(\mathbf{r})$ is the solute-solvent potential (input function), β is the inverse temperature, while $B_i(h-c)$ is the so called bridge function depending on the difference $\gamma_i = h_i - c_i$, the later functional dependence is also input data.

Therefore, the IET of molecular liquids is formulated in the 3D format as a search of

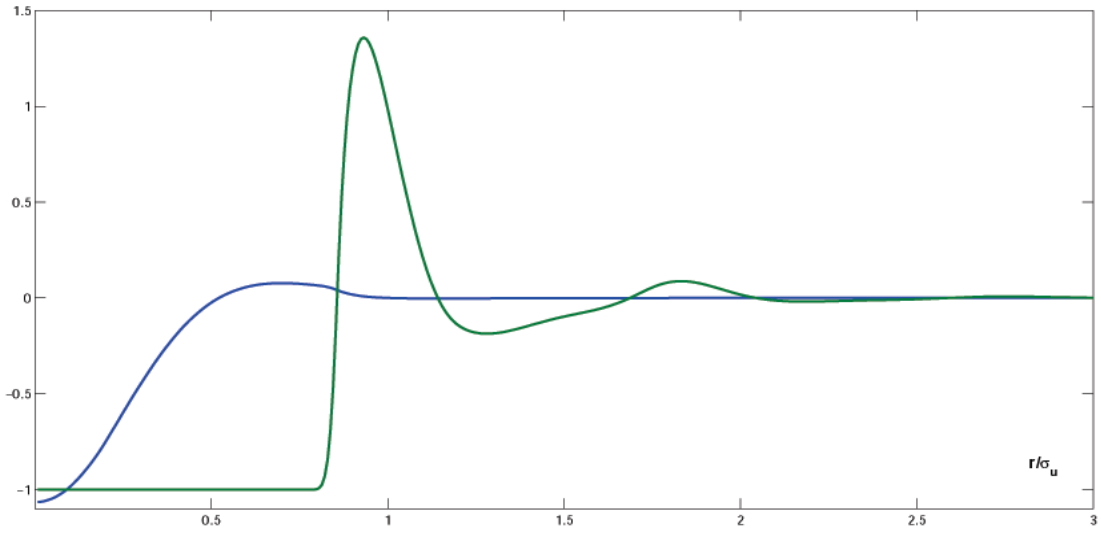

FIG. 1: The OZ and the DFT kernels, the green line corresponds to the nonlocal part of oxygen-oxygen susceptibility $\tilde{\chi}_{OO}(r) = (\chi_{OO}(r) - \delta(r))/n_0^2$ of water under normal conditions, the blue one to the nonlocal part of second-order direct correlation function $\tilde{C}_{OO}(r) = 0.01 n_0 * [C_2(r) - \delta(r)]$ scaled by factor 100. All the functions are obtained by solution 1D RISM/HNC integral equations.

solution (1-2) at given $\chi_{ij}(\mathbf{r}), U_i(\mathbf{r}), B_i(\gamma_i)$, and β. In the most cases of interest, the interaction potential U_i is presented as a sum of multi-center spherical contributions, i.e. $U_i(\mathbf{r}) = \sum_j U_{ij}(\mathbf{r}_j - \mathbf{r}_i)$, usually these contributions have long range coulomb asymptotics:

$$U_{ij}(r_{ij} \to \infty) = q_i q_j / r_{ij}, \tag{3}$$

where q_i and q_j are the partial charges of the relevant species, while r_{ij} is the distance between these species. We note also that the susceptibility χ_{ij} is defined as a numerical 3D array, and the bridge B as an analytical smooth function. In the general case the correlation functions have rather complicated shapes and behave differently at short-range and long-range distances. At short-range distances the functions reveal pronounced sharp peaks and slopes, whereas the functions decay weakly with oscillations at the long-range distances. Details of the distant dependence will be outlined below. The angular dependence of the sought-for functions are less investigated, it is known only that the dependence is smooth in most cases of the interest.

Peculiarities of the distance behavior of the correlation functions. We focus on the distant dependence of the sought-for functions and consider their behavior for the 3D

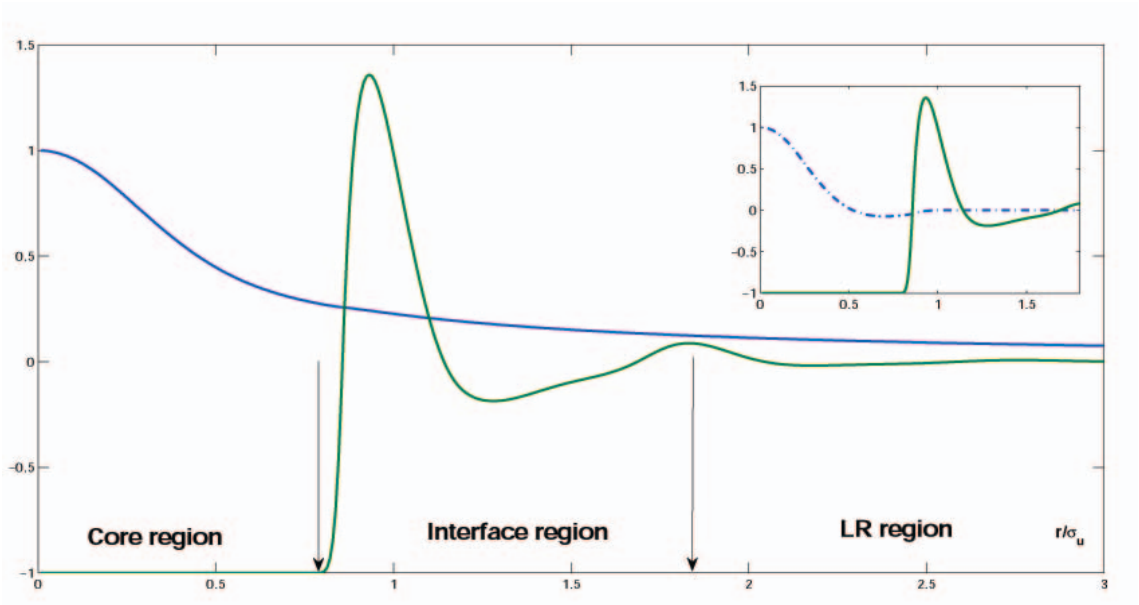

FIG. 2: The distance behavior of correlation functions, the green line corresponds to the total correlation function $h_{OO}(r)$ of water under normal conditions, the blue one to the relevant direct correlation function $\tilde{c}_{OO}(r) = c_{OO}(r)/c_{OO}(r=0)$. The inset shows the similar behavior of short-range direct correlation function $\tilde{c}_s(r) = [c_{OO}(r) + \beta U(r)]/c_{OO}(r=0)$ in the core the interface regions.

format, since the angular averaging does not affect this behavior. First, we note that kernel $\chi(\mathbf{r})$ has complicated behavior (see Fig. 1), it oscillates at large distances weakly decaying. The scale σ_v of the oscillations is determined by the real part of the first pole of the fourier transform $\mathcal{F}(\chi) = \int \exp[i\mathbf{kr}]\chi(\mathbf{r})d\mathbf{r}$. The decay scale σ_d is typically larger by a factor of 4-5.

The direct correlation function $c(\mathbf{r})$ decreases rapidly at distances less than size σ_u determined by an increase of the potential $U(r \to 0)$ (see Fig. 2). We denote this region as the core ($r < \sigma_u$). At the same time, the direct correlation function $c(\mathbf{r})$ is quite close to $-\beta U$ at $r > \sigma_u + \sigma_v$. We define this region as a linear response (LR) region, since it can be easily obtained from the OZ equation that $h \to -\beta\chi * U$ in the region, (where symbol $*$ means convolution integration). We can obtain the asymptotical behavior of the total correlation functions from the closure relation:

$$h(r \to 0) = -1. \tag{4}$$

Moreover, the transition to the short-range limit $r \to 0$ occurs rapidly at $r < \sigma_u$. The function $h(\mathbf{r})$ rises sharply at distances above σ_u and typical scale of these changes is about

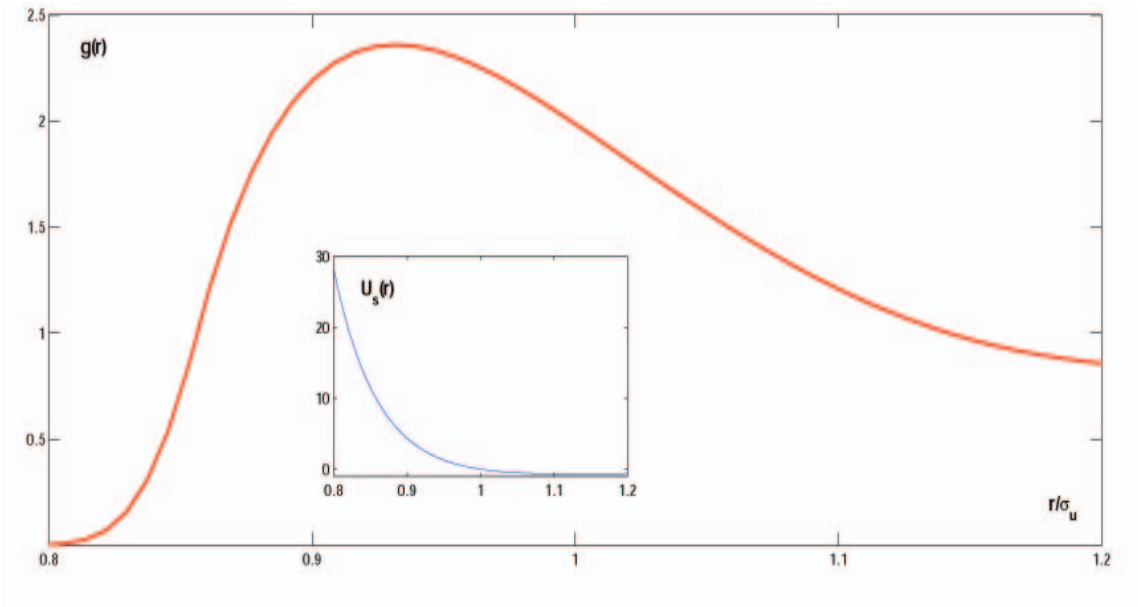

FIG. 3: The distance behavior of $g_{OO}(r)$ in the region of the exponential growth. The inset shows the similar behavior of the interaction potential $U(r)$ at the same region.

of $ds = 0.05\sigma_u$ (Fig. 3). We refer the region ($\sigma_u < r < \sigma_u + \sigma_v$) as the interface region. On the other hand, the total correlation function $h(\mathbf{r})$ oscillates at large distances weakly decaying, the scales of oscillations and decay are mainly determined by the first pole of the function χ. Thus, we have three domains (the core, the interface, and the LR regions) in which the behavior of correlation functions is quite different (see, Fig.2).

III. IET IN TERMS OF SOLVENT INDUCED POTENTIAL

Variational formulation of IET. Below we focus on the 3D format, the extension to the 6D and 1D consideration is straightforward. Following the density functional theory for nonuniform molecular liquids[14] we consider the density functional of the free energy $A(n(\mathbf{r}))$ determined by the relation:

$$\beta A(n_i(\mathbf{r})) = \sum_i \int n_i(\mathbf{r})(\ln[\frac{n_i(\mathbf{r})}{n_0}] + \beta U_i(\mathbf{r}) - 1)d\mathbf{r}$$
$$-\frac{1}{2}\int\int \sum_{ij} \Delta n_i \cdot \mathbb{C}_{ij}(\mathbf{r}-\mathbf{r}', n_i) \cdot \Delta n_j(\mathbf{r}')d\mathbf{r}d\mathbf{r}', \quad (5)$$

where $n_i(\mathbf{r})$ is the density distribution of solvent sites of type i around the solute, while $\Delta n_i(\mathbf{r}) = n_i(\mathbf{r}) - n_0$ is the change in this distribution, and n_0 is the average density of

the solvent. This distribution is related with the relevant correlation functions $h_i(\mathbf{r})$ as $n_i(\mathbf{r}) = n_0(h_i(\mathbf{r}) + 1)$. In the above equation, the matrix $\mathbb{C}_{ij}(\mathbf{r} - \mathbf{r}', n_i)$ is the second order direct correlation function, which functional dependence on n_i is not known in the general case. However, we may relate $\mathbb{C}_{ij}(\mathbf{r}-\mathbf{r}', n_i)$ with the similar function of pure solvent $\mathbb{C}^0_{ij}(\mathbf{r}-\mathbf{r}')$ (see Fig. 1) while the later can be expressed in terms of solvent susceptibility:

$$\mathbb{C}_{ij}(\mathbf{r} - \mathbf{r}', n_i) = \mathbb{C}^0_{ij}(\mathbf{r} - \mathbf{r}') + \Delta\mathbb{C}_{ij}(\mathbf{r} - \mathbf{r}', n_i) \qquad \mathbb{C}^0_{ij}(\mathbf{r}) = \delta_{ij}\delta(\mathbf{r})/n_0 - \chi^{-1}(\mathbf{r}). \tag{6}$$

The above free energy functional $A(n(\mathbf{r}))$ corresponds to the general formulation of 3D solvation problem, however a successive application of the functional to molecular liquids depends on the appropriate choice of the functional dependence $\Delta\mathbb{C}_{ij}(n_i)$. If this dependence is known, then the calculation of functional derivative $\mathbb{C}'_{ijk} = \delta\Delta\mathbb{C}_{ij}/\delta n_k$ is straightforward. We do not focus here on this problem and will discuss it elsewhere. The minimization of the free energy functional $A(n(\mathbf{r}))$ with respect to $n(\mathbf{r})$ leads to the nonlinear integral relations

$$\ln[h_i(\mathbf{r}) + 1] = -\beta U_i(\mathbf{r}) + h_i(\mathbf{r}) - \sum_j \chi^{-1}_{ij} * h_j + B_i(\mathbf{r}), \tag{7}$$

where we introduce the bridge function $B_i = \sum_{jk} \Delta n_j * \mathbb{C}'_{ijk} * \Delta n_k/2$. In this paper we assume $B = 0$ that corresponds to the so called hypernetted chain closure (HNC). We note that eq. (7) can be transformed to the closure relation by the substitution $c_i(\mathbf{r}) = \sum_j \chi^{-1}_{ij} * h_j(\mathbf{r})$, while the inverse form of the later equation leads to the 3D OZ integral equation. Therefore, the free energy functional (5) provides the variational formulation of the IET for molecular liquids.

Solvent induced potential. We introduce new variables $u_i(\mathbf{r})$, which refer to as solvent induced potential (SIP):

$$u_i(\mathbf{r}) = \ln[h_i(\mathbf{r}) + 1]/\beta + U_i(\mathbf{r}). \tag{8}$$

The SIP has physical meaning, it is related with the mean-force potential $W_i(\mathbf{r}) = u_i - U_i$, and with change in the excess chemical potential $\Delta\mu_i(\mathbf{r})$ caused by insertion of the solute in the position $\mathbf{r}$ from the i-th solvent site:[15]

$$u_i(\mathbf{r}) = \mu_i + \mu_u - \Delta\mu_i(\mathbf{r}), \tag{9}$$

where μ_i and μ_u are excess chemical potentials of the i-th solvent site and solute, respectively.

Manipulation with the SIP has some advantages with respect to the conventional treatment of the IET of molecular liquids, since

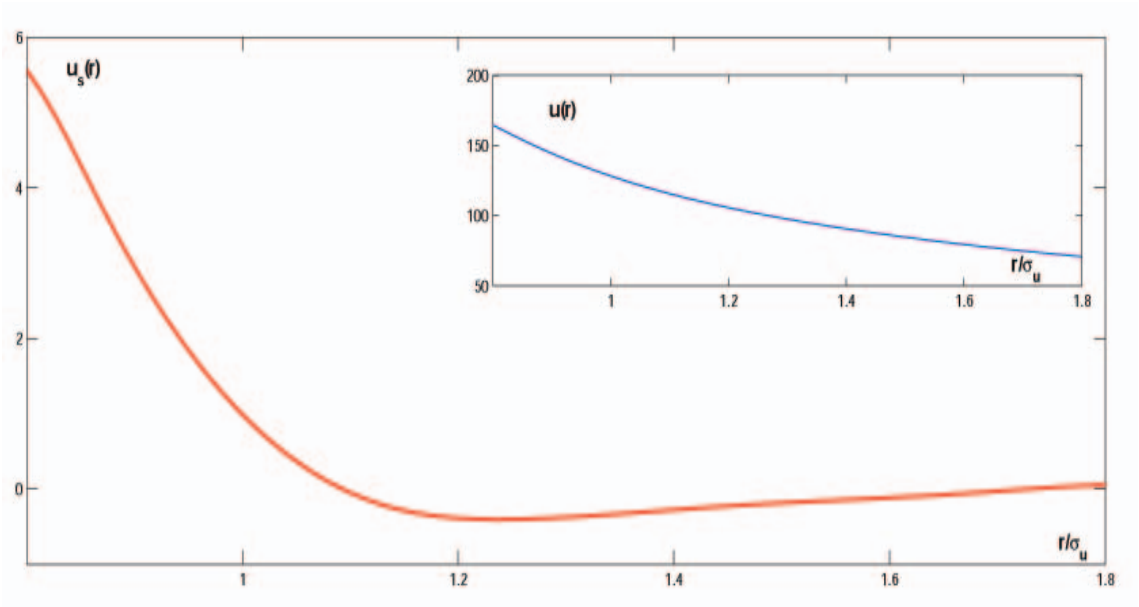

FIG. 4: Distance behavior of $u^s(r)$ of the oxygen-oxygen SIP for water under normal conditions in the interface region. The inset shows the similar behavior of the relevant $u(r)$.

a) in contrast to h and c the SIP is a smooth function without any sharp changes (see Fig. 4);

b) data on the SIP are enough to calculate both h and c, while knowledge of functions h and c is not enough to evaluate the SIP;

c) the free energy functional is quadratic for certain closure approximations like as HNC, and partially linearized HNC.

IET in terms of SIP. The IET can be rewritten in terms of the SIP as the linear integral equations (when the function h is known):

$$\beta u_i(\mathbf{r}) = \mathbb{C}_{ij} * h_j. \tag{10}$$

This reformulation allows us to account asymptotical behavior of the correlation function h. For this purpose, we consider the zero approximation $h_i^0(\mathbf{r})$ of this function by introducing the Mayer function

$$f_i(\mathbf{r}) = \exp[-\beta U_i(\mathbf{r})] - 1. \tag{11}$$

Then we define $h_i^0(\mathbf{r})$ as

$$h_i^0(\mathbf{r}) = \exp[-\beta U_i(\mathbf{r}) + \mathbb{C}_{ij} * f_j] - 1. \tag{12}$$

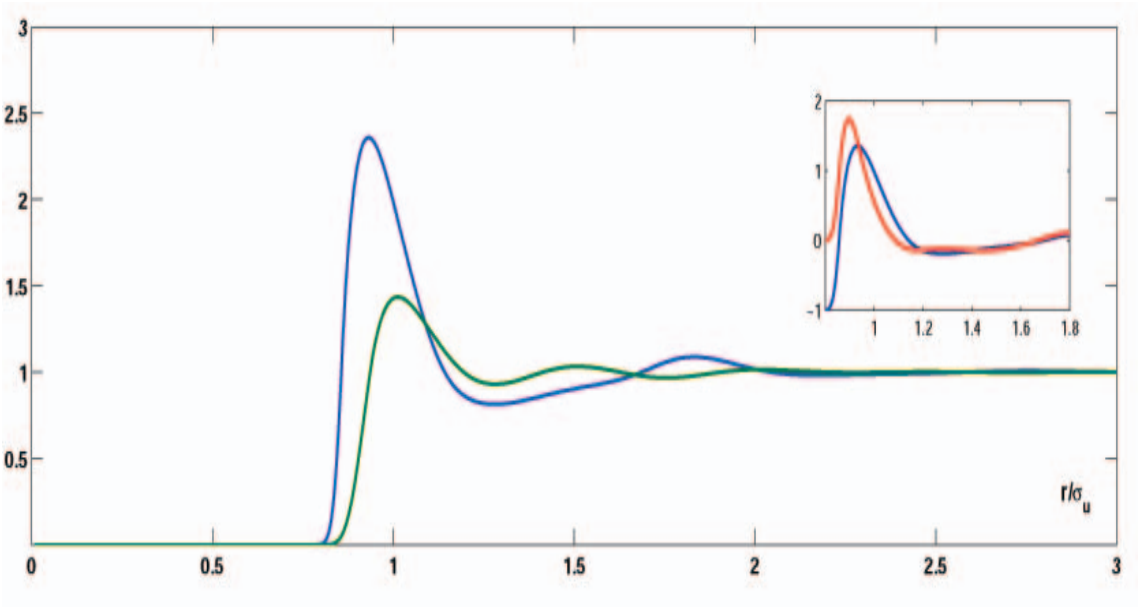

FIG. 5: The distance behavior of $h(r)$ (blue curve) and $h^0(r)$ (green curve) of the oxygen-oxygen for water under normal conditions. The inset shows the similar behavior for $h(r)$ (blue curve) and residue $h(r) - h^0(r)$ at the interface region.

This approximation can be easily evaluated before solution of integral equations. Moreover this approximation reveals all the peculiarities of asymptotical behavior of h, it is quite close to -1 below σ_u, and corresponds to the linear response in the LR region. The difference between $h_i^0(\mathbf{r})$ and $h_i(\mathbf{r})$ is significant only in the narrow interface region (Fig. 5). Therefore, using the substitution

$$\beta\Delta u_i(\mathbf{r}) = \beta u_i(\mathbf{r}) - \mathbb{C}_{ij} * h_j^0, \tag{13}$$

we reduce the problem to the evaluation of the SIP residue in the interface region

$$\beta\Delta u_i(\mathbf{r}) = \mathbb{C}_{ij} * [h_j - h_j^0] = \mathbb{C}_{ij} * \Delta h_j \tag{14}$$

We will show below that the evaluation of the SIP in the core region is straightforward when the SIP is known for interface region.

Solvent induced potential and the Poisson-Boltzmann equation. The kernel $\mathbb{C}_{ij}^0$ reveals a complicated distant dependent behavior. But, it can be split in the short-range ($\mathbb{C}_{ij}^s$) and the long range parts as

$$\mathbb{C}_{ij}^0(\mathbf{r}) = \mathbb{C}_{ij}^s(\mathbf{r}) - \frac{\beta q_i q_j}{r_{ij}}. \tag{15}$$

Then introducing the electrostatic potential $\psi(\mathbf{r})$ as

$$\psi(\mathbf{r}) = \sum_j \int_{\mathbf{R}^3} \frac{q_j n_j(\mathbf{r}_1) d\mathbf{r}_1}{|\mathbf{r} - \mathbf{r}_1|}, \tag{16}$$

we may also split the short-range and the long-range part of the SIP:

$$u_i(\mathbf{r}) = u_i^s(\mathbf{r}) + q_i \psi(\mathbf{r}). \tag{17}$$

The short-range contribution $u_i^s(\mathbf{r})$ is to be calculated by the integral equation:

$$\beta u_i^s(\mathbf{r}) = \mathbb{C}_{ij}^s * h_j, \tag{18}$$

while the integral equation for electrostatic potential $\psi(\mathbf{r})$ can rewritten in the differential (local) form:

$$\nabla^2 \psi(\mathbf{r}) = 4\pi \sum_j q_j n_j(\mathbf{r}). \tag{19}$$

The last relation is the Poisson-Boltzmann (PB) equation,[16] whereas various approximations used for n_j and u^s to evaluate integral in (16) result in the so-called nolocal electrostatic approach.[17] Therefore, we conclude $u_i(\mathbf{r})$ to be a change in the electrochemical potential, while u^s and ψ are its non-electrostatic and electrostatic contributions. Although the relation between u_i and the Poisson-Boltzmann equation is known, the incorporation of the short-range part u_i^s is not straightforward and has been provided only for very simply models.[18]

In the general case, the algorithms for calculations of u_i^s and ψ are to be different, because they have distinct long-range asymptotical behavior. There are several approaches for solutions to the PB equation based on wavelets, multigrid, or multiscale methods (see, review[8]). Below, we will focus on methods for evaluations of the short-range part u^s, while the evaluations of the electrostatic potential will be considered in a separate paper.

IV. IET IN THE BASIS SET REPRESENTATION

Approximation of sought-for functions. To describe the main idea, we omit below solvent indexes (considering a monoatomic liquid). The extension of the proposed algorithms to the case of molecular liquids and nonzero bridge is straightforward, we should consider matrices instead relevant vectors, tensors instead of the relevant matrices, etc.

Let's us expand the sought-for functions u (the index s is also omitted below) and h in an orthogonal basis set $\mathbf{a}(\mathbf{r}) = \{a_1(\mathbf{r}), a_2(\mathbf{r}), ..., a_{N_s}(\mathbf{r})\}$ whose dimension is N_n:

$$\Delta u(\mathbf{r}) = \sum_{s=1}^{N_s} \hat{u}_s a_s(\mathbf{r}) = \hat{\mathbf{u}} \cdot \mathbf{a}, \qquad \Delta h(\mathbf{r}) = \sum_{s=1}^{N_s} \hat{h}_s, a_s(\mathbf{r}) = \hat{\mathbf{h}} \cdot \mathbf{a} \tag{20}$$

where $\mathbf{a}$ is the vector of the basis functions, while $\hat{\mathbf{h}}$ and $\hat{\mathbf{u}}$ are the vectors of the approximating coefficients for the corresponding sought-for functions, while symbol $\cdot$ means the scalar product. Then, the integral equation (18) can be rewritten in the matrix form for the approximating coefficients

$$\beta \hat{\mathbf{u}} = \hat{\mathbb{C}} \cdot \hat{\mathbf{h}}, \tag{21}$$

where $\hat{\mathbb{C}}$ is the matrix which elements C_{ij} are obtained by double integration

$$C_{ij} = \int_{\mathbf{R}^3} \int_{\mathbf{R}^3} a_i(\mathbf{r}) C(\mathbf{r} - \mathbf{r}_1) a_j(\mathbf{r}_1) d\mathbf{r} d\mathbf{r}_1. \tag{22}$$

Therefore, the problem can be reduced to the iterative solution of the matrix equation

$$\beta \Delta \hat{\mathbf{u}}^{(n+1)} = \hat{\mathbb{C}} \cdot \hat{\mathbf{h}}^{(n)}, \tag{23}$$

while the n-th iteration of function $h(\mathbf{r})$ is expressed in terms of vectors $\mathbf{a}$ and $\hat{\mathbf{u}}^{(n)}$:

$$h^{(n)}(\mathbf{r}) = \exp[-\beta(U(\mathbf{r}) + \hat{\mathbf{u}}^{(n)} \cdot \mathbf{a})] - 1. \tag{24}$$

Hence, we may propose the following iterative scheme: a) initial stage: fast evaluation of matrix $\hat{\mathbb{C}}$ and vector $\hat{\mathbf{h}}^0$ with the use of a basis set and further storage of these arrays in a memory, b) iterative solution of (23) and (24). Formally, this stage can be written as

$$\hat{\mathbf{u}}^{(n)} \to (24) \to h^{(n)} \to (20) \to \hat{\mathbf{h}}^{(n)} \to (23) \to \hat{\mathbf{u}}^{(n+1)}. \tag{25}$$

Of course, there are a lot of ways to provide such iteration, but we outline an approach which naturally account properties of the sought-for functions, namely, their smoothness, localization, and asymptotical behavior.

Reduction of the 3D integrals to evaluations in the interface region. We divide the whole volume into the core, the interface, and the LR regions, i.e.

$$\mathbf{R}^3 = \mathbf{V}_{cr} \cup \mathbf{V}_{ir} \cup \mathbf{V}_{lr}. \tag{26}$$

Since the difference $h(\mathbf{r}) - h^0(\mathbf{r})$ is nonzero only in the interface region, then calculations of the integrals can be reduced only to evaluations in this region. We remark that this region includes only 1-2% of mesh points used in the uniform FFT (see Fig.6). Thus, we reduce the complexity of computational costs by 50 times.

V. CONSTRUCTION OF REAL SPACE MESH FOR 3D SOLVATION

Domain decomposition with the use of solvent accessible surface. First, we should decompose the interface region to provide the required integration with high effectiveness. The concept of solvent accessible surface (SAS) can be applied to perform such decomposition. The SAS has been introduced to calculate free energy of hydrophobic solutes.[19] The meaning of the SAS is the following. The hydrophobic solute can be presented as a collection of hard spheres with van-der-Waals radii. When rolling a sphere, representing a solvent molecule, over the van der Waals surface of the solute, we can construct the SAS as the locus of points swept out by the center of the solvent sphere.[20] The free energy of the hydrophobic solutes is assumed to be proportional to SAS. Now, this concept is widely used to built SAS and other molecular surfaces around biomacromolecules. There are effective tools[21] which are able to perform fast calculations of the SAS as well as the first and the second derivatives of the SAS with respect to atomic coordinates. Typically the computation of SAS require the number operations which is linearly (for small solutes) or quadratically (for large solutes) proportional to the number of the solute atoms.

Of course, we can not reduce volume integrals to the evaluation of a SAS, but we may split the interface region into the few scaled SASs and reduce the problem to the evaluation of surface integrals. Thus, the interface region can be presented as a collection of spherical shell elements (SSE) build from relevant parts of scaled SASs (see, Fig. 7). Each SSE represents a set of scaled SAS elements (SE). Such construction is supposed to decrease significantly the computation of the volume integrals, because the angular dependence of the sought-for functions in each SSE is to be very weak. Therefore, we perform the following division of the interface region:

$$\mathbf{V}_{ir} = \mathbf{V}_1 \cup \mathbf{V}_2 .... \cup \mathbf{V}_{N_{sse}}, \qquad \mathbf{V}_i = \mathbf{S}_{i1} \otimes \mathbf{dr} \cup \mathbf{S}_{i1} \otimes \mathbf{dr} ... \mathbf{S}_{iN_{se}} \otimes \mathbf{dr}, \tag{27}$$

where $\mathbf{V}_i$ is the volume of the i-th SSE, while $\mathbf{S}_{is}$ is a s-th scaled SAS which belongs to the i-th SSE. Due to that we can construct basis set as a union of basis sets $a_i^s(\mathbf{r})$ for each SSE, where the first index corresponds to the s-th SSE, while the second index indicate the i-th basis function for this SSE. Then, all the equations can be rewritten in terms of this union basis set.

Orthogonal polynomials and spherical harmonics as the optimal basis set. As we have indicated above, the variable $u(\mathbf{r})$ is a very smooth function. Its distance dependence

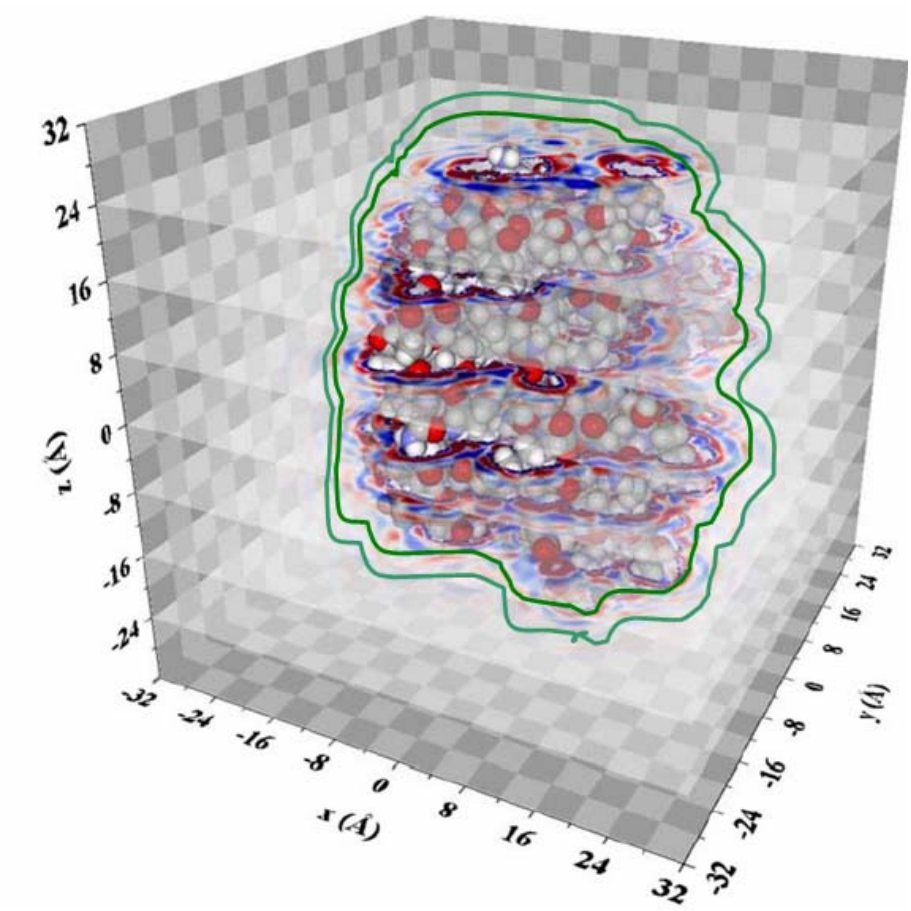

FIG. 6: Sketch of solvation in the interface region. The 3D distribution function of water oxygen around α-chymotripsinogen obtained in Ref.[22]. The grey cells correspond to the uniform mesh of size 128^3 used in the current IET algorithms. The solid green curves indicate boundaries of the interface region.

in the interface region seems to be approximated by low-order polynomials. It is expected their order does not exceed 6, since the SIP is 5-order piece-wise polynomial for the hard-sphere potential $U(r)$. The change of the hard-sphere potentials to the Lennard-Jones ones does not effect the polynomial order but only smooths the SIP behavior at the contact region $r \approx \sigma_u$ where derivative of the SIP is discontinues for the hard sphere potentials.

Thus, we may use the Chebyshev polynomials $T_k(r)$ to approximate distance dependence for each SSE. Since, the interaction potential U is a sum of spherical contributions, we may use spherical coordinates and apply the spherical harmonics $P_l^m(\theta, \phi)$ to approximate angular dependencies. Hence, we construct the basis set as a product of the Chebyshev

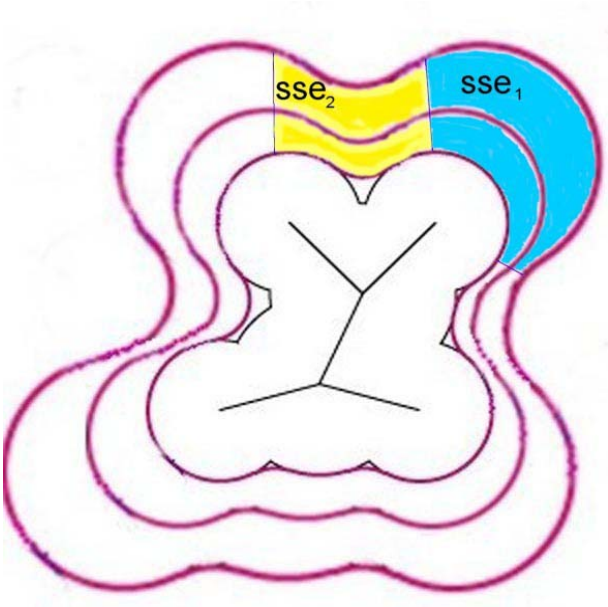

FIG. 7: Sketch of domain decomposition of the intreface region. The violet curves depict scaled SAS, the blue and the yellow regions correspond to spherical shell elements consisting from patches of the corresponding SAS.

polynomials and spherical harmonics

$$a^s_{kml}(\mathbf{r}) = T_k(|\mathbf{r} - \mathbf{r_s}|)P^m_l(\cos\theta)\exp[im\phi]. \tag{28}$$

We denote this basis set $\mathbf{a}^s(\mathbf{r})$ as the tensor product of the orthogonal polynomials and spherical harmonics

$$\mathbf{a}^s = \mathbf{a}^s_T \otimes \mathbf{a}^s_P, \tag{29}$$

where $\mathbf{a}^s_T$ and $\mathbf{a}^s_P$ are respective subsets consisting of the polynomials and the harmonics. Then, we can rewrite matrix eq. (21) in the tensor form:

$$\hat{\mathbf{u}}^s = \hat{\mathbf{u}}^s_T \otimes \hat{\mathbf{u}}^s_P, \qquad \hat{\mathbf{u}}^s_T = \hat{\mathbf{h}}^s_T \cdot \hat{\mathbb{C}}_T, \qquad \hat{\mathbf{u}}^s_P = \hat{\mathbb{C}}_P \cdot \hat{\mathbf{h}}^s_P. \tag{30}$$

where $\hat{\mathbf{u}}^s_J$ is the vector of the approximating coefficients of the $J-$the subset ($J = T, P$) while $\hat{\mathbb{C}}_T$ and $\hat{\mathbb{C}}_P$ are the matrices whose elements are equal to of the scalar product of the kernel and the respective basis functions.

It is important that due to construction of the SSE the angular dependency of the total correlation function h is very simple for each SSE and may be approximated by few spherical

harmonics, whereas the angular dependence of the kernel is very complicated for each SSE. However, the complexity of calculations of the scalar product $\hat{\mathbf{h}}_P^s \cdot \hat{\mathbb{C}}_P$ would be determined by $\dim(\hat{\mathbf{h}}_P^s)$ not $\dim(\hat{\mathbb{C}}_P)$. On other other hand, the radial dependence of h is not smooth in the core region in contrast to the that of the kernel, therefore the complexity of calculations of the scalar product $\hat{\mathbf{h}}_T^s \cdot \hat{\mathbb{C}}_T$ is to be determined by $\dim(\hat{\mathbb{C}}_T) << \dim(\hat{\mathbf{h}}_T^s)$. Thus, we can cut off the approximations of the radial dependence of h and the angular dependence of $\hat{\mathbb{C}}$ and account only the few approximating coefficients of them.

VI. EFFECTIVE CALCULATIONS OF THE KERNEL

Evaluation of kernel in the tensor product approximation. In the general case, the kernel $\mathbb{C}(\mathbf{r}-\mathbf{r}')$ is degenerate, i.e. it can be expressed as a product[23]

$$\mathbb{C}(\mathbf{r}-\mathbf{r}_1) \approx \sum_{n=1}^{N_{max}} y_n(\mathbf{r}) \cdot x_n(\mathbf{r}_1). \tag{31}$$

To prove it, we use the Taylor expansion:

$$\mathbb{C}(\mathbf{r}-\mathbf{r}_1) = \sum_{n=1}^{\infty} \mathbf{r}_1^n \cdot \nabla^n \frac{\mathbb{C}(\mathbf{r})}{n!}. \tag{32}$$

However, the function $C(\mathbf{r})$ is smooth outside the region of exponential growth (which is very narrow, see inset in Fig. 2). Hence, this function has only few nonzero derivatives and may be well approximated by few number of piece-wise polynomials with an accuracy proportional to scale of the region of exponential growth. For examples, in the case of hard-sphere potentials U the function C is to be the third-order polynomial.[24] Thus, we my reduce infinite sum (32) to evaluations of few first terms by (31). Then, the matrix $\hat{\mathbb{C}}$ can be also decomposed as the tensor product, i.e.

$$\hat{\mathbb{C}} = \hat{\mathbb{L}} \cdot \hat{\mathbb{R}}, \qquad \hat{\mathbb{L}} = \mathbf{a} \otimes \mathbf{r}^n, \qquad \hat{\mathbb{R}} = \mathbf{f}_n \otimes \mathbf{a}, \tag{33}$$

where $\mathbf{f}_n = \nabla^n \mathbf{C}(\mathbf{r})/n!$, and elements of matrices $\hat{\mathbb{L}}$ and $\hat{\mathbb{R}}$ are 3D integrals (not 6D as $\hat{\mathbb{C}}$):

$$L_i^{n[s]} = \int_{\mathbf{V}_s} \mathbf{r}^n a_i^s(\mathbf{r}) d\mathbf{r}, \qquad R_i^{n[s]} = \int_{\mathbf{V}_s} \mathbf{f}_n(\mathbf{r}) a_i^s(\mathbf{r}) d\mathbf{r}. \tag{34}$$

Moreover, the matrix $\hat{\mathbb{L}}$ includes evaluations of the few first moments of the basis functions and it is independent on the input data. Therefore, using orthogonal polynomials as the basis

set, we may reduce strongly the dimension of the basis from N_s down to N_{max} corresponding to the number of nonzero derivatives of the kernel.

At the same time, we need only to modify $\hat{\mathbb{L}}$ for calculations of SIP in the core region and construct it from elements. The elements of matrix $\hat{\mathbb{L}}$ are to be modified as

$$\tilde{L}_i^{n[s]} = \int_{\mathbf{V}_{cr}} \mathbf{r}^n a_i^s(\mathbf{r}) d\mathbf{r}. \tag{35}$$

Therefore, we reduce the problem to the evaluations the SIP in the interface region.

Application of the fast spherical Fourier transform and fast polynomial transforms. We reduce the problem to the evaluation of volume integrals on each SSE. These integrals are to be calculated by consequent integration over the shell surfaces and the shell widths. Both the integration procedures may be accelerated by the non-equispaced FFT (NFFT).[25] In the case of the surface integration we may use the fast spherical Fourier transforms (see for example Ref.[26]). In the general there are several methods to provide it, (see, for example discussions in[27,28]), depending on the choice of nodes (arbitrary or special grid), applying discrete cosine transform or fast multipole methods, etc. We suppose to use the standard discretization of the sphere surface, consisting of all pairs of the form (θ_l, ϕ_m) with $cos(\theta_i)$ $(0 \leq i \leq 2l-1)$ being the Gauss-Legendre quadrature nodes of degree $2l$ and ϕ_m being equispaced on the interval $[0; 2\pi]$. It has been shown[26,27] what the computational complexity of such calculations may be decreased down to $O(l_m^2 \ln l_m)$ where l_m is the so called bandwidth of the approximated functions. As we estimate above, the bandwidth l_m is to be about of $\dim(\hat{\mathbf{h}}_P^s)$. On the other hand, an effective summation over different scaled SAS which belong to the same SSE can be provided by the fast discrete polynomial transform,[29] which is also has computational complexity $O(N_r \ln N_r)$, where N_r is the number of the scaled SAS of each SSE. We cas estimate N_r as $N_r \approx \dim(\hat{\mathbb{C}}_T)$. Thus, the total complexity of the fast computation is about of $O(N_{SSE} * \dim(\hat{\mathbb{C}}_T) * \dim^2(\hat{\mathbf{h}}_P^s) \ln[\dim(\hat{\mathbb{C}}_T) + \dim(\hat{\mathbf{h}}_P^s)]$, where N_{SSE} is the total number of SSE which is to be about of number of solvent accessible atoms. We expect $\dim(\hat{\mathbb{C}}_T) < 4$ and $\dim(\hat{\mathbf{h}}_P^s) < 3$ to be enough to provide a reasonable accuracy of calculations in most of cases.

VII. DISCUSSION AND SUMMARY

Using correlation functions derived from the linear response theory as an initial guess, we reduce the 3D solvation problem to evaluations of the SIP residue $\Delta u(\mathbf{r})$ in the narrow interface region. Due to such consideration, we reduce the number N_{grid} of grid points by 2 orders. However, effective RSM techniques are to be applied to provide the similar reduction of the computational complexity of the problem. In general, various basis set representations can used for it. The curvlets[30], multidimensional splines,[31] and multivariate orthogonal polynomials are the most popular approaches in the 3D case. We choose orthogonal polynomials, since the sought-for functions are very smooth and may be well approximated by low-order polynomials. The Chebyshev series seems to be most suitable for the 3D solvation problem, since the Chebyshev polynomials can provide FFT in a bounded interval. It allows us to apply NFFT and reduce the computational complexity to the value $N_{grid} \ln N_{grid}$. If we increase the number of finite elements by an additional subdivision of SSE, we can apply B-splines instead of polynomials and perform NFFT in a way similar to that proposed in Ref.[32] However, we believe the proposed approach to be a reasonable balance between complexity caused by the complicated shape of molecular solutes and smoothness of the sought-for functions. The domain decomposition of the interface region in terms of SSE built form patches of SAS can provide a further reduction of the computational complexity. We assume to use the tensor decomposition of the kernel for non-contacted SSE. Such decomposition allows us to apply the Fast Multipole Method and decrease the computational complexity to $N_s \ln N_s$, where N_s is the number of grid points for two neighboring SSE. We suppose the total complexity of the computation to be about of $\dim(\hat{\mathbb{C}}_T) * \dim^2(\hat{\mathbf{h}}^s_P) \ln[\dim(\hat{\mathbb{C}}_T) + \dim(\hat{\mathbf{h}}^s_P)]$, while the total number of the SSE can vary from units up to thousands. Therefore, the computational complexity can be reduced down to 10^3 for small organic solutes and to 10^4 for biomacromolecules instead of $8 * 10^6$ and of $8 * 10^7$ provided respectively by current algorithms based on the uniform FFT.[33,34]

Summary Starting from the free energy functional for the 3D solvation problem, we reformulate the IET of molecular liquids in terms of the solvent induced potential. It allows us to reduce the problem to evaluation of the volume integrals in the interface region. Then, we perform a domain decomposition of the region in terms of spherical shell (finite) elements consisting from of the relevant surface elements. These surface elements are built

from scaled solvent accessible surfaces. We suppose to use the NFFT or the tensor product approximation for fast evaluation of the kernel. The computational complexity of the calculations are assumed to be reduced by 10^3 times with respect to current algorithms of the molecular solvation, which are based on the uniform FFT.

VIII. APPENDIX. OVERVIEW OF IET OF MOLECULAR LIQUIDS

Full molecular (6D) Format. For a homogeneous molecular liquid the MOZ equation is written by:[12]

$$h(\mathbf{r},\mathbf{\Theta}) = \int_{\mathbf{R}^3}\int_{\mathbf{\Theta}} \chi(\mathbf{r}-\mathbf{r}_1,\mathbf{\Theta}-\mathbf{\Theta}_1)c(\mathbf{r}_1,\mathbf{\Theta}_1)d\mathbf{r}_1 d\mathbf{\Theta}_1, \tag{36}$$

where $\mathbf{\Theta}$ contains all possible orientations of a molecule, $\mathbf{\Theta} = \{(\psi,\theta,\phi) \mid \psi \in [0,2\pi],\ \theta \in [0,\pi],\ \phi \in [0,2\pi]\}$, while the solvent susceptibility function $\chi(\mathbf{r},\mathbf{\Theta})$ describes the mutual correlations of the sites of solvent molecules in the bulk solvent. This function is the input data of the problem in the case of infinitely diluted solution. The MOZ equation must be complemented with a closure relationship, which is an additional equation that relates $h(\mathbf{r},\mathbf{\Theta})$ with $c(\mathbf{r},\mathbf{\Theta})$. The general form is the closure relation is written as

$$h(\mathbf{r},\mathbf{\Theta}) = \exp[-\beta U(\mathbf{r},\mathbf{\Theta}) + h(\mathbf{r},\mathbf{\Theta}) - c(\mathbf{r},\mathbf{\Theta}), + B(h-c)] - 1 \tag{37}$$

where $U(\mathbf{r},\mathbf{\Theta})$ is the solute-solvent potential (input function), β is the inverse temperature, while $B(h-c)$ is the bridge function depending on the difference $\gamma = h - c$, the later functional dependence is also input data. At the current level the MOZ can be solved only for rather symmetrical type of potential U.

Reduced (1D RISM) Format. The conventional approximation is to reduce the dimensionality by averaging the functions over angular distributions. It is performed by averaging the susceptibility around solvent sites. Then, we have a set of three-dimensional (3D) susceptibilities $\chi_{ij}(\mathbf{r})$ instead of 6D susceptibility, i.e. $\chi(\mathbf{r},\mathbf{\Theta}) \approx \chi_{ij}(\mathbf{r})$:

$$\chi_{ij}(\mathbf{r}) = \frac{1}{4\pi}\int_{\mathbf{\Theta}} \chi(\mathbf{r}+\mathbf{r}_{ij},\mathbf{\Theta})d\mathbf{\Theta}, \tag{38}$$

where $\mathbf{r}_{ij}$ is the shift vector, when we rotate solvent site j around solvent site i. Then, we obtain the integral equations in 3D format (see Sec.2).

The further reduction my be obtained by averaging the functions around solute sites

$$c_{ij}(r) = \frac{1}{4\pi}\int_{\mathbf{\Omega}} c_i(\mathbf{r}+r_j)d\mathbf{\Omega}, \tag{39}$$

where Ω is the solid angle defined by orientation of vector $\mathbf{r}_j$. The model is referred to as 1D reference interaction site model (1DRISM),[35] for which the OZ equations are given by

$$h_{ij}(r) = \sum_{s=1}^{N_u}\sum_{m=1}^{N_v}\int\limits_{R^3}\int\limits_{R^3} \omega_{is}(|\mathbf{r}-\mathbf{r}'|)c_{sm}(|\mathbf{r}'-\mathbf{r}''|)\chi_{mj}(r'')d\mathbf{r}'d\mathbf{r}'', \tag{40}$$

where N_u is the number of solute sites (in the general case, it may exceeds hundreds and even thousands for macromolecular solutes), $\omega_{ij}(r)$ is the intramolecular correlation function written as

$$\omega_{ij}(r) = \delta_{ij} + [1-\delta_{ij}]\frac{\delta(r-r_{ij})}{4\pi r_{ij}^2}, \tag{41}$$

where r_{ij} is the distance between the solute sites, and $\delta(r-r_{ij})$ is the Dirac delta-function. The reduction of the closure relation is similar, we need to replace only the sought-for 6D functions by the relevant distant dependent matrices. Within the framework of 1D RISM approach the solute and solvent molecules are modeled as a set of sites interacting via pairwise distance dependent potentials $U_{ij}(r)$. Thus, the input functions are the following $\omega_{ij}(r), \chi_{ij}(r), U_{ij}(r), B_{ij}(\gamma)$, and β. Again, the averaging increases the size of the sought-for functions transforming them into matrices, but strongly decreases the dimensionality of the integrals. Although, the complete treatment of (40) required 6-fold integration, application of the fourier transform reduces it to a set of linear equation for the relevant fourier transforms.

Iterative scheme of the solution. In this subsection we omit the distance and the angular dependencies of the sought-for functions, because the scheme of the solution of integral equation is the same for the 1D, the 3D, and even the 6D format. In all these cases, the equations are solved by an iterative scheme. Combining the OZ and the closure equations, it can be easily obtained the recurrent relation between $n+1$ and n iterations:

$$\mathcal{F}(h^{(n+1)}) = \mathcal{F}(\chi)\cdot[\mathcal{F}(h^{(n)}) - \mathcal{F}(\ln[h^{(n)}+1]+\beta U)]. \tag{42}$$

Unfortunately, this relation can be hardly used, because function $\ln(h+1)+\beta u$ is ill defined at small distances. However Eq. (42) can be rewritten in terms of new variable $\gamma = h - c$ (referred to as indirect correlation function) and expressed as

$$\mathcal{F}(\gamma^{(n+1)}) = \mathcal{F}(\chi)\cdot[\mathcal{F}(\exp[-\beta U+\gamma^{(n)}]-1) - \mathcal{F}(\gamma^{(n)})]. \tag{43}$$

Therefore, the conventional algorithm for solution of the integral equations is based on the fast fourier transform (FFT), whereas the iterative scheme can be schematically written by

$$\gamma^{(n)} \to FFT \to \mathcal{F}(\gamma^{(n)}) \to OZ \to \mathcal{F}(\gamma^{(n+1)}) \to IFFT \to \gamma^{(n+1)}, \tag{44}$$

where $IFFT$ means inverse fast fourier transform. The conventional algorithms are based on the 1D and the the 3D FFT for the 1D and 3D RISM respectively. All the current algorithms apply a uniform grid. The required number of grid points is about $N_g = \sigma_d/ds > 500$ for the 1D RISM, whereas this value rises up to $N_g^3 \approx 10^8$ for the 3D RISM, since the cartesian grid is usually used. The application of NFFT instead of FFT is not simple, because the function γ has a complicated multi-scale behavior, it oscillates at large distances like as h, has a region in which it rises sharply (exponentially). Moreover, the region of the exponential growth is very narrow (about $0.03\sigma_u$) and very sensitive to changes in the input data (potential U and susceptibility χ).

---

[1] For recent reviews, see: Cramer, C.; Truhlar, D., Chem. Rev. 99, 2161 (1999).

[2] Bashford, D.; Case, D., Annu. Rev. Phys. Chem. 51, 129 (2000).

[3] J. Tomasi, B. Mennucci and R. Cammi, Chem. Rev. 105 2999 (2005).

[4] see, for example: van Gunsteren, W.; Berendsten, H., Angew. Chem., Int. Ed. Engl. 29, 992 (1990).

[5] Vaidehi, N.; Wesolowski, T.; Warshel, A., J. Chem. Phys. 97, 4264 (1992).

[6] F. Hirata, Molecular Theory of Solvation (Springer, Berlin, 2003).

[7] Holst M; Saied F, J. Comput. Chem. 14, 105 (1993).

[8] Beck TL, Rev. Mod. Phys. 72, 1041 (2000).

[9] Frink LJD; Salinger AG, J. Comput. Phys. 159, 407 (2000); Frink LJD; Salinger AG; Sears MP; et al.; J. Phys. Cond. Matter 14, 12167 (2002).

[10] Chuev GN; Fedorov MV, J. Chem. Phys. 120, 1191 (2004); J. Comput. Chem. 25, 1369 (2004).

[11] M. P. Sears and Laura J.D. Frink, J. Comput. Phys. 190, 184 (2003).

[12] J.-P. Hansen, I. R. McDonald, Theory of Simple Liquids (Academic Press, London, 2006).

[13] D.S. Palmer, G.N. Chuev, E.L. Ratkova and M.V. Fedorov, Curr. Pharm. Design 17, 1695 (2011).

[14] Chandler D; Mccoy JD; Singer SJ, J. Chem. Phys. 85, 5971 (1986).

[15] Lee LL; Shing KS, J. Chem . Phys. 91, 477 (1989).

[16] Boschitsch, A. H.; Fenley, M. O., J. Comput. Chem. 25, 935 (2004); Shu-wen, W. C.; Honig, B., J. Phys. Chem. B 101, 9113 (1997); Misra, V. K.; Draper, D. E., J. Mol. Biol. 299, 813 (2000).

[17] A, A. Komyshev, in The Chemical Physics of Solvation, edited by R. R. Dogonadze, E. Kalman, A. A. Korynshev, and J, Ulstrup (Elsevier, Amsterdam, 1985).

[18] Bhuiyan, L. B.; Outhwaite, C. W., J. Colloid Interface Sci. 2009, 331, 543; Lue L; Zoeller N; Blankschtein D, Langmuir 15, 3726 (1999).

[19] Feig M; Brooks CL, Current opinion in structural biology 14, 217 (2004).

[20] Lee, B.; Richards, F. M., J. Mol. Biol. 55, 379 (1971).

[21] Connolly ML, J. Mol. Graphics 11, 139 (1993); Sridharan S; Nicholls A; Sharp KA, J. Comput. Chem. 16, 1038 (1995); Sanner MF; Olson AJ; Spehner JC, Biopolymers, 38, 305 (1996)); Tsodikov OV; Record MT; Sergeev YV, J. Comput. Chem. 23, 600 (2002).

[22] T. Imai, A. Kovalenko, F. Hirata, Chem. Phys. Lett. 395, 1 (2004).

[23] W. Hackbusch, Integral equations: theory and numerical treatment (Birkhäuser Verlag, Berlin, 1995).

[24] V. I. Kalikmanov, Statistical Physics of Fluids (Springer, Berlin, 2001).

[25] A. F. Ware, SIAM Rev. 40, 838 (1998).

[26] Kunis S; Potts D, J. Comput. Appl. Math. 161, 75 (2003).

[27] Tygert M. , J. Comput. Phys. 227, 4260 (2008)

[28] D.M. Healy, P.J. Kostelec, D. Rockmore, S.S.B. More, J. Fourier Anal. Appl. 9, 341 (2003).

[29] Potts D; Steidl G; Tasche M, Math. Comput. 67, 1577 (1998).

[30] Starck JL; Candes EJ; Donoho DL, IEEE Trans Image Proc. 11, 670 (2002).

[31] Arcangéli, R., Lòpez de Silanes, M.C., Torrens, J.J.: Multidimensional Minimizing Splines. Theory and Applications. Grenoble Science. (Kluwer Academic, Boston, 2004).

[32] Sammis I. and Strain J., J. Comput. Phys. 228, 7086 (2009).

[33] Gusarov, S.; Ziegler, T.; Kovalenko, A., J. Phys. Chem. A 110, 6083 (2006).

[34] M. C. Stumpe, N. Blinov, D. Wishart, A. Kovalenko, and V. S. Pande, J. Phys. Chem. B 115, 319, (2011).

[35] Chandler, D.; Andersen, H. C., J. Chem. Phys. 57, 1930 (1972).